

The Profile of Expression of SG2NAs Differs Between Cancer Types and it is Involved in the Reprogramming of Tumour Cell Proteome.

Padmini Bisoyi

JNU: Jawaharlal Nehru University

Padmalaya Devi

Acharya Harihar Regional Cancer Centre

Kusumbati Besra

Acharya Harihar Regional Cancer Centre

Anamika Prasad

JNU: Jawaharlal Nehru University

Buddhi Prakash Jain

MGCUB: Mahatma Gandhi Central University <https://orcid.org/0000-0002-7225-7257>

SHYAMAL GOSWAMI (✉ skg.lab220@gmail.com)

JNU: Jawaharlal Nehru University

Research Article

Keywords: SG2NA, STRIPAK, Striatin, Breast cancer, cell reprogramming.

Posted Date: December 8th, 2021

DOI: <https://doi.org/10.21203/rs.3.rs-1130676/v1>

License: © ⓘ This work is licensed under a Creative Commons Attribution 4.0 International License.

[Read Full License](#)

Abstract

Striatin and SG2NA are scaffold proteins that form signalling complexes called STRIPAK. It has been associated with cancer and other diseases. Our earlier studies have shown that SG2NA forms a complex with the cancer-associated protein DJ-1 and signalling kinase Akt, promoting cancer cell survival. In the present study, we used bioinformatics analyses to confirm the existence of two isoforms of human SG2NA i.e., 78 and 87 kDa. In addition, several smaller isoforms like 35 kDa were also seen in western blot analyses of human cell lysates. The expression of these isoforms varies between different human cancer cell lines. Also, the protein level does not corroborate with its transcript level, suggesting a complex regulation of its expression. In breast tumour tissues, the expression of the 35 and 78 kDa isoforms was higher as compared to the adjacent normal tissues, while the 87 kDa isoform was detected in the breast tumour tissues only. With the progression of stages of breast cancer, the expression of 78 kDa isoform decreased, while 87 kDa became undetectable. In coimmunoprecipitation assay, the profile of SG2NA interactome in breast tumor vis-à-vis adjacent normal breast tissues shows hundreds of common proteins, while some proteins specifically interacted in breast tumour tissue only. We conclude that SG2NA is involved in diverse cellular pathways and has roles in cellular reprogramming during tumorigenesis.

Introduction

Striatin is the prototype member of a small subfamily of WD-40 repeat superfamily of proteins [1]. The other two members are SG2NA and Zinedin (also called Striatin 3 and 4 respectively). Besides the signature WD-40 repeats in their C-terminus, they are also characterized by one each of caveolin-binding, coiled-coil, and calmodulin-binding domains that are involved in protein-protein interactions [2]. Striatin-interacting phosphatase and kinase (STRIPAK) complexes are a group of multi-protein assemblies held together by the Striatin proteins as the scaffolds [3]. STRIPAK complexes are conserved in evolution, and they regulate diverse cellular processes viz., vesicular trafficking, Golgi assembly, Hippo signalling, autophagy, cell migration, cell cycle, cell differentiation, metabolism, and programmed cell death [3]. Dysfunctional STRIPAK assemblies have been associated with various developmental and degenerative diseases including cancer [4–6]. The protein phosphatase 2A (PP2A), a major regulator of the cellular phosphoproteome, is a dimer of the subunits A & C, that binds to the regulatory subunit B. There are four structurally distinct variants of the B subunit. Striatin & SG2NA are the organizers of the subunit B" in which they assemble several kinases and other proteins [7, 8].

Tumour progression and metastasis involves aberrant kinase signalling and cytoskeletal reorganization; and STRIPAKs have roles in both of these processes [4, 6]. Hippo signalling regulates organ size and tissue homeostasis, and dysfunctional Hippo signalling has often been associated with cancer. Serine-threonine kinases MST1 & 4 are the constituents of STRIPAK and in association with MOB, it contributes to the Hippo signalling [9, 10]. In prostate and hepatocellular carcinoma, increased expression of MST4 has been reported. It enhances the ERK signalling, and induces EMT [11]. MST3/4 are involved in the phosphorylation of Ezrin, Radixin, and Moesin (ERM proteins) that facilitate cell migration. Striatin-

interacting protein STRNIP2 antagonizes the functions of MST3/4 [12]. STRIPAK complexes are also involved in cytoskeletal reorganization in cancer cells. Actin-binding protein cortactin facilitates cancer cell invasion. Striatin binds to cortactin-binding protein CTTNBP2, suggesting its role tumorigenesis [13].

SG2NA, the second member of the Striatin family was initially isolated as a novel auto-antigen in the sera of a lung and bladder cancer patient [14]. Mouse SG2NA has at least six variants generated by alternate splicing, intron retention and RNA editing [15]. Variants of SG2NA are conserved in evolution, have similar but distinctive structural characteristics and are functionally related [16, 17]. Unlike Striatin that primarily expresses in the striatum region of the brain (and named accordingly), expression of SG2NA is more ubiquitous [15, 18, 19]. Our recent studies have suggested that SG2NAs have roles in certain cancer associated events like cytoskeletal reorganization, membrane sialylation, and modulation of the markers of EMT [20, 21]. Variants of SG2NA associate with the anti-oxidant protein DJ-1 and protects neuronal and cancer cells from oxidative stress [19, 22]. SG2NA also regulates ER homeostasis and the expression of 78 kDa SG2NA is modulated with the progression of cell cycle [23, 24]. In the present study, we have examined whether the profile of expression of SG2NA isoforms in cancer cell lines and biopsies can be related to the cancer type. Our study suggests that the expression of SG2NA is extensively modulated in several cancer cell lines and tissues; and it is involved in the reprogramming of the cellular proteome towards cancer phenotypes.

Materials And Methods

1. Cell culture

Different human cancer cell lines were procured from NCCS, Pune, India. Cells were cultured as a monolayer in 10% FBS containing DMEM with antibiotic penicillin, amphotericin B and streptomycin in a humidified, 5% CO₂ containing incubator at 37°C.

2. RNA extraction and RT-PCR

Total RNA was extracted from different cancer cell lines using TRI reagent. First strand cDNA was synthesized from 1 µg of RNA with reverse transcriptase (Epicentre) and oligo (dT)18 primer (Fermentas) at 37°C for 2 h. PCR was done using isoform specific primer pairs.

3. Preparation of cell/tissue lysates

Lysate (cells/tissue) was prepared in lysis buffer (50 mM Tris pH 7.6, 1 mM EDTA, 400 mM NaCl, 1 mM EGTA, 1% NP-40, 1 mM sodium orthovanadate, 10 mM sodium fluoride, protease and phosphatase inhibitor cocktail) and centrifuged at 4°C for 15 min @ 10,000 g. The supernatant was used for immunoblotting.

4. Western blotting

Estimation of protein concentration was done by modified Bradford method. Equal quantities of protein sample from each cell lines/tissue (70 µg) were resolved on 10% SDS-PAGE. The separated proteins were then transferred on PVDF membrane in Towbin's buffer (25 mM Tris, 192 mM glycine and 20% methanol). Membrane blocking was done for 2–3 h at room temperature in 5% BSA in 0.05% TBST buffer; then incubated overnight with primary antibody of SG2NA at 4°C. Immunodetection was done using HRP-conjugated mouse secondary antibody.

5. Southern blotting

PCR product was resolved on 1.5% agarose gel in 1X TAE buffer and immobilized on a nylon membrane. Prehybridization followed by probing with labelled Sg2na cDNA probe (double stranded, random labelled, 10^6 cpm/ml) overnight at 55°C. Filters were finally washed twice and developed.

6. Stability studies on Sg2na transcript

Transcription was inhibited by the treatment with actinomycin D (10 µg/ml). Cells were then harvested at different time points and RNA was extracted using TRI reagent, converted to cDNA. Sg2na transcripts were assayed by real time PCR using 1× SYBR Green, Sg2na ORF specific primers and 1 µl of cDNA. β-Actin transcript was used as an internal control.

7. Human Biospecimen

Human tissues used in the present study were collected from Acharya Harihar Regional Cancer Centre (AHRCC), Cuttack, from December 2018 to July 2019. An observational pilot study was done from the hospital data of patients with carcinoma of breast, colon and stomach. All patients were confirmed histopathologically and cases of primary tumors are included in this study. Altogether, 16 samples including 10, 3 and 3 patients of breast, colon and stomach carcinoma respectively were considered for the study. All the patients underwent surgery in AHRCC, Cuttack, followed by adjuvant treatment as indicated from postoperative histopathological features. The resected tissues were immediately collected and preserved immediately in liquid nitrogen for protein analysis. In this study respective clinical parameters like age, sex, clinical presentation, type of surgery, final detailed histopathology, TNM Staging and Stage Grouping were retrieved from hospital records (Supplemental Table S4). The final analysis of the study included comparison of the profile of SG2NA variants between adjacent normal and tumor tissues in all the cancer specimens.

8. Co-immunoprecipitation

The Protein G agarose beads were washed with 1X PBS on a rotary shaker for 5 mins followed by centrifugation at 13000g for 30 sec at room temperature. The washed beads were then equilibrated with filter sterile IP lysis buffer (20 mM Tris HCl pH 8, 137 mM NaCl and 1% Triton X-100, 2mM EDTA). The swollen beads were then resuspended in a certain volume of lysis buffer. Breast tissue lysates (both tumor and control) were prepared by incubating in IP lysis buffer, supplemented with protein inhibitor

cocktail and kept in ice for 1 hr followed by centrifuging at 12000g for 15 minutes. One milligram of each tissue lysate were added to the equilibrated beads and incubated for 2 hr at 4°C on rotatory shaker. Each lysate-beads mix was then centrifuged for 5 mins at 2000 rpm and supernatant were transferred into fresh tube. Each supernatant was added to the antibody crosslinked beads, mixed gently, followed by overnight incubation at 4°C on a rotatory shaker. Each supernatant was then removed by spinning at 13000 rpm for 30 sec at 4°C and the agarose pellet were resuspended in washing buffer (20 mM Tris HCl pH 7.4, 150 mM NaCl, 2 mM EDTA, 1% Triton X-100, 2mM EGTA, 0.2mM sodium orthovanadate) for 5 mins followed by centrifugation. This step was repeated five times with last wash in the same buffer without detergent. The bead bound immunocomplex were then resuspended in low pH Glycine buffer (0.1 M Glycine, pH 2) for 15 mins at 4°C. Each supernatant was then collected by centrifuging at 13000 g for 30 sec followed by neutralizing the protein mix by the adding 1.5 M Tris HCl (pH 8.8). This supernatant (pulled down proteins) was then collected for LC-MS analysis.

9. Sample Preparation for LC-MS/MS

25ul of sample was reduced with 5mM TCEP and further alkylated with 50mM iodoacetamide and then digested with Trypsin (1:50, Trypsin/lysate ratio) for 16 hr at 37° C. Digests were cleaned using a C18 silica cartridge to remove the salt and dried using speed vac. The dried pellet was resuspended in buffer A (5% acetonitrile, 0.1 formic acid).

10. Mass Spectrometric Analysis of Peptide Mixtures

All the experiments were performed using EASY-nLC 1200 system (Thermo Fisher Scientific) coupled to QExactive mass spectrometer (Thermo Fisher Scientific) equipped with Nano electrospray ion source. One microgram of the peptide mixture was resolved using a 25 cm Pico Frit column (360µm outer diameter, 75µm inner diameter, 10µm tip) filled with 1.9 µm of C18-resin (Dr Maeisch, Germany). The peptides were loaded with buffer A (5% acetonitrile, 0.1% formic acid) and eluted with a 0–40% gradient of buffer B (95% acetonitrile, 0.1% formic acid) at a flow rate of 300 nl/min for 100 min. MS data was acquired using a data-dependent top10 method dynamically choosing the most abundant precursor ions from the survey scan.

11. LC-MS/MS Data Processing

Samples were processed and RAW files generated were analysed with Proteome Discoverer (v2.2) against the Human UniProt reference proteome database. For Sequest and Amanda search, the precursor and fragment mass tolerances were set at 10 ppm and 0.02 Da, respectively. The protease used to generate peptides, i.e., enzyme specificity was set for trypsin/P (cleavage at the C terminus of “K/R: unless followed by “P”) along with maximum missed cleavages value of two. Carbamidomethyl on cysteine as fixed modification and oxidation of methionine and N-terminal acetylation were considered as variable modifications for database search. Both peptide spectrum match and protein false discovery rate were set to 0.01 FDR.

12. Bioinformatics analysis:

The protein list of interacting partners of SG2NA from co-immunoprecipitation in control and breast tumor tissue were analysed by BioVenn (biovenn.nl) comparison tool [25]. The protein-protein interaction network was analysed by STRING (Search Tool for the Retrieval of Interacting Genes/Proteins) tool. Functional enrichment of KEGG pathways (Kyoto Encyclopedia of Genes and Genomes) was done using STRING and DAVID (david.ncifcrf.gov) softwares [26, 27].

13. Ethical clearance:

All experimental protocols were approved by the Institutional Ethics Committee, AHRCC (IEC-AHRCC-065 dated 3rd July, 2018) and Institutional Ethics Review Board (IERB), JNU (IERB Ref No. 178/2018 dated 18th December, 2018). All the experiments were conducted under relevant guidelines and regulations. The consent was taken from each patient.

Results

Identification of the human variants of SG2NA: We have reported earlier that in mouse, there are at least six isoforms of SG2NA (87, 82, 78, 52 and 38 and 35 kDas) arising out of alternative splicing, intron retention and transcript editing [15, 18] Although SG2NA is highly conserved in evolution [17], its variants in human are not known. We analysed the EST and NCBI database (<https://blast.ncbi.nlm.nih.gov/Blast.cgi>) which predicted four transcript variants as shown in Fig. 1A. To validate the EST database, total RNA was isolated from HEK293T cells and RT-PCR was performed using primer pair flanking the intron region (forward, exon 5 and reverse, exon 15). In RT-PCR we obtained 2 bands of length around 1000-1200 bp (Fig. 1B). To confirm the identity of these bands, southern blotting was performed using full length human cDNA for *sg2na* (www.origene.com) as the probe. As shown in Fig. 1C, two distinct bands corresponding to 78 and 87 kDa variants (derived from the size of the RT-PCR products) were seen in the autoradiogram.

Further analysis was performed using UniProtKB/Swiss-Prot, Gene cards, and NCBI databases (<https://www.uniprot.org/>, <https://www.expasy.org/resources/uniprotkb-swiss-prot>, <https://www.genecards.org/>, <https://www.ncbi.nlm.nih.gov/gene>). Only two isoforms viz., 87 and 78 kDa were found at the protein level. Finally, analyses using Ensemble (<https://asia.ensembl.org/index.html>) and Gepia2 software (<http://gepia2.cancer-pku.cn/#index>), eight isoforms were mapped, out of which protein level expression were found for six isoforms (Table 1). One isoform i.e., STRN3-207 (332 aa) was found in the Uniprot and Ensemble database but it was predicted to undergo nonsense mediated decay [28, 29], hence it was not available in the EST database of NCBI. Three smaller isoforms i.e., STRN3-205, STRN3-206 and STRN3-208 appeared to be the fragments of the 78 and 87 kDa isoforms which might be formed by the proteolytic cleavage. Some other smaller isoforms (like the 35 and 52 kDa isoforms mouse) might be present in Human, but they could not be predicted by the bioinformatics analyses. As evident from all

analyses, we inferred that the two isoforms viz; 78 and 87 kDa are expressed in Human tissues at the protein level.

Table 1
Variants of SG2NA (STRN3*) as identified at the protein level from the Ensemble database (<https://asia.ensembl.org/index.html>).

Isoforms	Size	Exon and splicing status	Comments
STRN3-202	797 amino acids	All 18 exons	MW: 87 kDa,
STRN3-201	713 amino acids	Exons 8 and 9 are spliced	MW: 78 kDa
STRN3-206	112 amino acids	Consists of a part of exon 2, exon 3, 4 and part of exon 5	Fragment derived from the DNA sequence
STRN3-208	172 amino acids	Consist of only Exon 6, 7, 8 and 10	Fragment derived from the DNA sequence
STRN3-205	139 amino acids	Consist of only Exon 7, 9 and 10	Fragment derived from the DNA sequence
STRN3-207	332 amino acids.	Splicing of exon 8, 9 and 10 results in a premature stop codon. The transcript might undergo nonsense mediated decay	Nonsense mediated decay.
* In the data base, SG2NA is identified by Striatin 3 (STRN3).			

Expression profile of SG2NA variants differ among cancer cell lines

Earlier we have reported that in several cancer cell lines with increased levels of ROS; SG2NA recruits DJ-1 and phospho-Akt to the plasma membrane, promoting their survival and growth [19, 22]. To further analyse the role of SG2NA in cancer, we checked its expression in a number of well-studied human cell lines (Table 2). We first estimated the transcript level of *sg2na* in those cell lines. As shown in Fig. 2A, the level of *sg2na* mRNA was low in HepG2, H1293, and HeLa cells, moderate in A549 cells, and high in DU145 and HEK293T cells. Western analyses of the extracts from those cells however showed a different pattern (Fig. 2B). In HepG2 cells, the expression of 78kDa SG2NA was quite high and that of 87 kDa was low but detectable. In HeLa, DU145 and Hep3B cells, the expression of both 87 and 78 kDas was very low but detectable. In HEK293T, H1299 and A549 no expression was detected. Therefore, there were major incompatibilities between the mRNA and protein levels In HepG2 cells, the transcript level was the lowest, but the protein level was the highest. Contrastingly, in HEK293 and A549 cells, while the transcript levels were high, there were hardly any expression of the protein. To address this issue, we measured the stability of *sg2na* transcript in HEK293T, A549 and HepG2 cells. Cells were treated with actinomycin D, an inhibitor of transcription; and harvested at different time points post treatment. Total RNA was isolated

and *sg2na* mRNA level was estimated by qRT-PCR. As shown in Fig. 2C, in all the cell lines tested, *sg2na* transcript level decreased and reached to ~40-60% of the original level by 8 hours. However, it was more stable in A549 cells as the rate of decrease was < 25% in first 4 hours. This corroborates with the observation that the level of *sg2na* mRNA was higher in A549 cells than in HepG2 cells. Such post-transcriptional decay thus showed a complex mode of regulation of SG2NA at both mRNA and protein levels in different cell lines.

Table 2
Different human cell lines used in the study and their characteristics:

Name	Characteristics (https://www.atcc.org/)
1. HEK293T	Derived from human embryonic kidney 293 cells and contains the SV40 T-antigen.
2. A549	Generated through explant culture of lung carcinomatous tissue from a 58-year-old Caucasian male.
3. H1299	Established from the lymph node metastasis of the lung from a patient.
4. HepG2	Derived from a liver hepatocellular carcinoma of a 15-year-old Caucasian male.
5. Hep3b	Hepatoma cell line derived from the biopsies taken during lobectomies of an 8 year old black male.
6. DU145	Human prostate cancer cell line derived from a 69-year-old white male.
7. HeLa	First immortalized cell line to be developed from a 30-year-old black female suffering from aggressive cervical cancer.

Breast, gastric/stomach, and colon cancer tissues show distinctive expression profile of SG2NAs

Invasive and infiltrating ductal carcinoma are the most common form of breast cancer. We analysed four samples along with their normal counterparts (from the same patient collected from the adjoining region) by western blotting. As shown in Fig. 3, in all four samples, higher expression of 78 kDa and 35 kDa isoforms (not identified by bioinformatics analysis but it is predicted as it is present in mouse) of SG2NA were seen in tumour tissues as compared to normal counterparts. Noticeably, the 87 kDa isoform is expressed in tumour only. It is also found that with the increase in the stages of cancer, the expression of 78 kDa isoform decreases and that of 87 kDa isoform almost disappears in the 3rd stage. Much change was not seen in case of 35 kDa isoform. Details of the patients and the results is given in Table 3.

Adenocarcinoma is the most common type of stomach cancer comprising about 90% of all cases. It originates in the mucosa cells present in the innermost layer of the stomach that produce the mucus. We collected three samples and the details are given in Table 4. In the cases of the stomach carcinoma, each patient showed a different pattern of expression of SG2NAs (Fig. 3). It might be due to the heterogeneity of stomach tissues and the associated subtypes of adenocarcinoma. We also analysed the profile of SG2NA in three cases of colon cancer. However, unlike in the cases of breast and stomach, in the case of colon (both diseased and normal counter parts), the expression of SG2NA was quite low (Fig. 3) and no specific pattern was evident.

Table 3
Details of the breast cancer samples (Details given in Supplemental Table S4)

Total No. of cases used for the study = 10	Case 1: 15383	Case 2: 15327	Case 3: 15216	Case 4: 15215
Patient Age	48	45	44	50
BR Score	7	6	6	6
Histological grade of cancer	2	2	2	2
Stage of Cancer	2(A)	3(A)	3(A)	2 (A)
TMN classification	T3 N0 M0	T3 N1 M0	T3 N1 M0	T2 N0 M0
Profile of SG2NA:				
Case I: Higher expression of 87, 78 & 35kDa isoforms are found in tumor as compared to both Near and Far normal tissues. Two distinct bands (unidentified isoforms) are found in both tumor and normal (Near and Far) tissues. Several other bands (unidentified isoforms) are also seen in tumor only.				
Case II: Higher expression of 87, 78 & 35kDa isoforms are found in tumor as compared to both Near and Far normal tissues. Two distinct bands (unidentified isoforms) are found in both tumor and normal (Near and Far) tissues.				
Case III: Higher expression of 87, 78 & 35kDa isoforms are found in tumor as compared to both Near and Far normal tissues. Two distinct bands (unidentified isoforms) are found in both tumor and normal (Near and Far) tissues.				
Case IV: Higher expression of 87, 78 & 35kDa isoforms are found in tumor as compared to both Near and Far normal tissues. Two distinct bands (unidentified isoforms) are found in both tumor and normal (Near and Far) tissues.				

Table 4

Details of the stomach/gastric cancer samples (Details given in Supplemental Table S4)

Total no. of cases used for the study = 3	Case1: 15355	Case 2: 15324	Case 3: 15312
Patient Age (in years)	75	62	40
Patient Disease	Adenocarcinoma of Stomach (Mucinous and Signet ring cell type)	Adenocarcinoma of Stomach (Mixed tubular and Dysplasia type)	Adenocarcinoma of Stomach (Tubular type)
Grade of Cancer	III	III	III
Stage of Cancer	3B	2B	2B
TMN classification	T4 N2 M0	T4 N2 M0	T4 N2 M0
Profile of SG2NA:			
Case I: Higher expression of 35kDa isoform in both Near and Far normal tissues as compared to the tumor. 87kDa isoform is expressed only in Near normal tissue. Tumor shows high expression of high molecular weight isoform of SG2NA in the form of a smear			
Case II: The Far normal tissue express 35kDa isoform while the near normal tissue does not show expression of any major isoforms. Tumor tissue expresses both 87kDa and 35kDa isoforms.			
Case III: Both Far and Near normal tissue expresses both 87 and 35kDa isoforms. Tumor tissue expresses low level of 35kDa isoform			

The interactome of SG2NA in breast tumour and its normal counterparts partially overlap

As described above, in the breast cancer tissues there were modulations in the expression of the variants of SG2NA, although no definitive pattern was evident. Since SG2NAs are scaffold proteins, to probe into their potential functions in cancer, we looked into their interacting partners. Lysates were prepared from normal and breast tumour tissues from the same patient, coimmunoprecipitated with the SG2NA antibody, followed by LC-MS/MS. Total 215 and 291 proteins were immunoprecipitated from the normal and the tumour tissues respectively. Among those, 187 proteins were common between both, 104 were found only in tumour tissue and 28 were found only in the normal counterpart (details given in Supplemental Table S1 and Fig. 4). In the functional enrichment analysis for KEGG pathways, we found that the interacting partners of SG2NA present in both normal and tumour tissues are involved in diverse biological functions including metabolism; cell structure; protein synthesis and processing; neurodegenerative, cardiovascular and infectious diseases; cell signalling; etc. (Supplemental Table S2). Similar analyses of the interacting partners of SG2NA found only in tumour tissues also showed their involvement in diverse pathways but those were not directly related to breast cancer (except oestrogen signalling, Supplemental Table S2). Upon comparison, we found that (i) Many interacting proteins common between normal and tumour tissues are involved in cancer related pathways viz., HIF-1 signalling, Tight/Gap junction, Pentose phosphate pathway, function of the ER etc., though they were not

exclusive for the tumour sample (Supplemental Table S2). (ii) In the pathways that were common between the normal & tumour samples vis-à-vis the tumour only samples, certain proteins were found in the tumour samples only, but they were the isoforms of those found in the common pool (e.g., while ENO-1 and PGK-1 were present in the common pool; ENO-2/3 and PGK-2 were found in the tumour only pool; Supplemental Table S2). (iii) There were eighteen pathways that were exclusive for the tumour tissues but none except spliceosome, oestrogen signalling, and viral oncogenesis have been directly related to cancer (Supplemental Table S3). We then analysed the functions of 104 proteins that were found only in tumor samples and as shown in Table 5, most of them have been reported as the prognostic markers for various types of cancers. The significance of this analyses is discussed in the following section.

Table 5

Details characteristics of the interacting partners of SG2NA found in breast tumor tissues only (<https://www.proteinatlas.org>).

Gene name	Protein Name	Function	Relation to cancer
Mitochondrial function			
1. ATP50	Subunit of ATP synthase	ATP synthesis, Hydrogen ion transport	Prognostic marker in renal cancer (favorable)
2. RPS25	Mitochondrial ribosomal protein L22		Not prognostic
3. COA6	Cytochrome c oxidase assembly factor 6	Mitochondrial respiration	Prognostic marker in renal cancer (unfavorable) and urothelial cancer (favorable)
Complement pathway			
4. CLU	Clusterin	Apoptosis, Complement pathway, Innate immunity	Prognostic marker in thyroid cancer (favorable)
5. C4BPA	Complement component 4 binding protein alpha	Complement pathway/Innate immunity	Prognostic marker in endometrial cancer (favorable) and liver cancer (favorable)
6. C4A	Complement C4A	Systemic lupus erythematosus,	Not prognostic
7. C5	Complement C5	Complement pathway/Innate Immunity/Inflammatory response	Prognostic marker in liver cancer (favorable)
8. C3	Complement C3	Age-related macular degeneration, Hemolytic uremic syndrome,	Prognostic marker in renal cancer (unfavorable) and liver cancer (favorable)
Structural Protein			
9. CLTC	Clathrin heavy chain	Autophagy, Cell cycle/division/mitosis	Prognostic marker in urothelial cancer (unfavorable), liver cancer (unfavorable), cervical cancer (unfavorable) and colorectal cancer (favorable)
10. FGA	Fibrinogen alpha chain	Amyloidosis, Cancer-related gene	Prognostic marker in renal cancer (unfavorable) and liver cancer (favorable)

Gene name	Protein Name	Function	Relation to cancer
11. MYH10	Myosin heavy chain 10	Actin/Calmodulin-binding, Motor protein	Prognostic marker in renal cancer (favorable) and urothelial cancer (unfavorable)
12. PFN1	Profilin 1	Actin binding	Prognostic marker in renal cancer (unfavorable)
13. TAGLN	Transgelin	Actin binding	Prognostic marker in renal cancer (unfavorable)
14. FSCN1	Faschin actin binding protein	Actin binding	Prognostic marker in renal cancer (unfavorable), lung cancer (unfavorable) and head and neck cancer (unfavorable)
15. CAPZB	F-actin-capping protein subunit beta	Actin capping, Actin binding	Prognostic marker in renal cancer (favorable) and liver cancer (unfavourable)
16. CTTNBP2NL	CTTNBP2 N-terminal-like protein	Actin dynamic	Prognostic marker in colorectal cancer (favorable) and renal cancer (favourable)
17. A2M	Alpha-2-macroglobulin	Cancer-related gene	Not prognostic
18. THBS1	Thrombospondin 1	Heparin-binding, Cell adhesion	Prognostic marker in renal cancer (unfavorable) and stomach cancer (unfavorable)
19. VTN	Vitronectin	Cell adhesion, Cancer-related genes	Prognostic marker in renal cancer (unfavorable) and liver cancer (favorable)
20. DSC3	Desmocollin	Cell adhesion	Prognostic marker in urothelial cancer (unfavorable)
21. POSTN	Periostin	Cell adhesion	Prognostic marker in renal cancer (unfavorable), lung cancer (unfavorable) and stomach cancer (unfavorable)
Metabolism			

Gene name	Protein Name	Function	Relation to cancer
22. DLST	Dihydrolipoamide S-succinyltransferase	TCA cycle	Prognostic marker in renal cancer (favorable)
23. ENO2	Enolase 2	Glycolysis, Cancer-related genes	Prognostic marker in renal cancer (unfavorable), liver cancer (unfavorable) and colorectal cancer (unfavorable)
24. ENO3	Enolase 3	Glycolysis	Prognostic marker in colorectal cancer (unfavorable)
25. PGK2	Phosphoglycerate kinase 2	Glycolysis	Not prognostic
26. PKLR	Pyruvate kinase L/R	Glycolysis	Not prognostic
27. TKT	Transketolase	Transketolase	Prognostic marker in liver cancer (unfavorable)
28. TXN	Thioredoxin	Antioxidant	Prognostic marker in endometrial cancer (favorable)
Protein synthesis			
29. EEF1A2	Eukaryotic translation elongation factor 1 alpha 2	Protein biosynthesis, GTP binding	Prognostic marker in endometrial cancer (unfavorable) and head and neck cancer (unfavorable)
30. EIF4A2	Eukaryotic translation initiation factor 4A2	Protein synthesis, RNA binding;	Not prognostic
31. EEF1A1	Eukaryotic translation elongation factor 1 alpha 1	Protein biosynthesis, Transcription,	Prognostic marker in liver cancer (unfavorable)
32. EEF1G	Eukaryotic translation elongation factor 1 gamma	Protein biosynthesis	Not prognostic
33. EIF3I	Eukaryotic translation initiation factor 3 subunit I	Protein biosynthesis	Prognostic marker in renal cancer (unfavorable), endometrial cancer (favorable) and liver cancer (unfavorable)
34. FAU	ubiquitin like and ribosomal protein S30 fusion	Ribosomal protein	Not prognostic
35. RPL7	Ribosomal protein L7	Ribosomal protein	Not prognostic

Gene name	Protein Name	Function	Relation to cancer
36. RPL7A	Ribosomal protein L7a	Ribosomal protein	Prognostic marker in ovarian cancer (unfavorable) and liver cancer (unfavorable)
37. RPL10	Ribosomal protein L10	Ribosomal protein	Prognostic marker in renal cancer (unfavorable)
38. RPL10L	Ribosomal protein L10 like	Ribosomal protein	Not prognostic
39. RPL13	Ribosomal protein L13	Ribosomal protein	Prognostic marker in endometrial cancer (favorable) and renal cancer (unfavorable)
40. RPL13A	Ribosomal protein L13a	Ribosomal protein	Prognostic marker in renal cancer (unfavorable) and liver cancer (unfavorable)
41. RPL18	Ribosomal protein L18	Ribosomal protein	Prognostic marker in renal cancer (unfavorable)
42. RPL22	Ribosomal protein L22	Ribosomal protein	Not prognostic
43. RPL24	Ribosomal protein L24	Ribosomal protein	Prognostic marker in renal cancer (unfavorable) and thyroid cancer (favorable)
44. RPL27	Ribosomal protein L27	Ribosomal protein	Prognostic marker in renal cancer (unfavorable)
45. RPL29	Ribosomal protein L29	Ribosomal protein	Not prognostic
46. RPLP2	Ribosomal protein lateral stalk subunit P2	Ribosomal protein	Prognostic marker in renal cancer (unfavorable) and liver cancer (unfavorable)
47. RPS3A	Ribosomal protein S3A	Ribosomal protein	Prognostic marker in liver cancer (unfavorable)
48. RPS16	Ribosomal protein S16	Ribosomal protein	Not prognostic
49. RPS11	Ribosomal protein S11	Ribosomal Protein	Prognostic marker in renal cancer (unfavorable)
Nucleic acid binding			

Gene name	Protein Name	Function	Relation to cancer
50. HNRNPA2B1	Heterogeneous nuclear ribonucleoprotein A2/B1	Ribonucleoprotein, RNA-binding	Prognostic marker in liver cancer (unfavorable), renal cancer (unfavorable) and prostate cancer (unfavorable)
51. HNRNPA1L2	Heterogeneous nuclear ribonucleoprotein A1-like 2	Packaging of pre-mRNA/ transport of mRNA/splice site selection.	Prognostic marker in breast cancer (favorable) and pancreatic cancer (favorable)
52. HNRNPA1	Heterogeneous nuclear ribonucleoprotein A1	mRNA processing/splicing/ transport	Most cancer tissues show moderate to strong nuclear staining. Not prognostic.
53. NCL	Nucleolin	DNA/RNA-binding	Prognostic marker in liver cancer (unfavorable) and endometrial cancer (unfavorable)
54. HNRNPA3	Heterogeneous nuclear ribonucleoprotein A3	Trafficking of RNA/ Pre-mRNA splicing	Prognostic marker in renal cancer (unfavorable), liver cancer (unfavorable) and cervical cancer (favorable)
Chaperone, Heat shock Protein			
55. HSPA1L	Heat shock protein family A (Hsp70) member 1 like	Molecular chaperone, cancer related gene	Prognostic marker in ovarian cancer (favorable) and renal cancer (favorable)
56. HSPA6	Heat shock protein family A (Hsp70) member 6	Molecular chaperone, stress response	Prognostic marker in renal cancer (unfavorable) and liver cancer (unfavorable)
57. HSP90AA1	Heat shock protein 90 alpha family class A member 1	Molecular chaperone, Cancer-related genes	Prognostic marker in renal cancer (favorable), liver cancer (unfavorable) and breast cancer (unfavorable)
58. HSPA2	Heat shock protein family A (Hsp70) member 2	Chaperone, cancer related gene	Prognostic marker in breast cancer (favorable) and lung cancer (unfavorable)
59. CCT3	Chaperonin containing TCP1 subunit 3	Chaperone	Prognostic marker in liver cancer (unfavorable) and renal cancer (unfavorable)

Gene name	Protein Name	Function	Relation to cancer
60. CCT7	Chaperonin containing TCP1 subunit 7	Chaperone	Prognostic marker in liver cancer (unfavorable) and endometrial cancer (unfavorable)
Immunity			
61. HLA-A	Major histocompatibility complex, class I, A	Adaptive & Innate immunity	Prognostic marker in ovarian cancer (favorable) and endometrial cancer (favorable)
62. HLA-B	Major histocompatibility complex, class I, B	Adaptive & Innate immunity	Prognostic marker in melanoma (favorable)
63. HLA-C	Major histocompatibility complex, class IC	Adaptive & Innate immunity	Not prognostic
Transport			
64. RAB1A	RAB1A, member RAS oncogene family	Autophagy, ER-Golgi transport, Protein transport	Prognostic marker in head and neck cancer (unfavorable)
65. RAB5A	Member, RAS oncogene family	Endocytosis, Phagocytosis, Protein transport	Not prognostic
66. RAB5B	Member RAS oncogene family	Protein transport	Prognostic marker in breast cancer (unfavorable)
67. RAB5C	Member RAS oncogene family	Protein transport	Prognostic marker in head and neck cancer (unfavorable)
68. SLC25A4	Solute carrier family 25 member 4	Host-virus interaction, Transport	Prognostic marker in renal cancer (favorable) and pancreatic cancer (favorable)
69. SLC25A6	Solute carrier family 25 member 6	Apoptosis, Transport	Not prognostic
70. NASP	Nuclear autoantigenic sperm protein	Cell cycle, DNA replication and protein transport	Prognostic marker in renal cancer (unfavorable), liver cancer (unfavorable) and melanoma cancer (unfavorable)
Nucleotide binding			

Gene name	Protein Name	Function	Relation to cancer
71. ARF4	ADP ribosylation factor 4	GTP-binding, Nucleotide-binding	Prognostic marker in liver cancer (unfavorable) and thyroid cancer (unfavorable)
72. ARF5	ADP ribosylation factor 5	GTP-binding, Nucleotide-binding,	Not prognostic
73. TUBB1	Tubulin beta 1 class VI,	GTP-binding, Nucleotide-binding	Gene product is not prognostic
74. TUBB2B	Tubulin beta 2B class IIb;	GTP-binding, Nucleotide-binding;	Prognostic marker in endometrial cancer (unfavorable)
75. TUBB4A	Tubulin beta 4A class IVa;	GTP-binding, Nucleotide-binding;	Prognostic marker in endometrial cancer (unfavorable)
76. TUBB6	Tubulin beta 6 class V;	GTP-binding, Nucleotide-binding	Prognostic marker in renal cancer (unfavorable) and urothelial cancer (unfavorable)
77. TUBB3	Tubulin beta 3 class III	GTP-binding, Nucleotide-binding;	Not prognostic
78. TUBB	Tubulin beta class I	GTP-binding, Nucleotide-binding;	Prognostic marker in renal cancer (unfavorable) and liver cancer (unfavorable)
79. TUBB4B	Tubulin beta 4B class IVb	GTP-binding, Nucleotide-binding;	Prognostic marker in thyroid cancer (favorable), endometrial cancer (favorable) and liver cancer (unfavorable)
80. TUBB2A	Tubulin beta 2A class IIa	GTP-binding, Nucleotide-binding	Prognostic marker in urothelial cancer (unfavorable) and renal cancer (favorable)
81. TUBB8	Tubulin beta 8 class VIII;	GTP-binding, Nucleotide-binding;	Not prognostic
Signalling			

Gene name	Protein Name	Function	Relation to cancer
82. YWHAB	Tyrosine 3-monooxygenase/tryptophan 5-monooxygenase activation protein beta	Signalling, cancer related	Prognostic marker in liver cancer (unfavorable), renal cancer (favorable), endometrial cancer (unfavorable), lung cancer (unfavorable), head and neck cancer (unfavorable) and breast cancer (unfavorable)
83. YWHAQ	Tyrosine 3-monooxygenase/tryptophan 5-monooxygenase activation protein theta	Signalling	Prognostic marker in liver cancer (unfavorable) and endometrial cancer (unfavorable)
84. YWHAZ	Tyrosine 3-monooxygenase/tryptophan 5-monooxygenase activation protein zeta	Signalling	Prognostic marker in renal cancer (unfavorable), pancreatic cancer (unfavorable), liver cancer (unfavorable), endometrial cancer (unfavorable) and lung cancer (unfavorable)
85. STRN	Striatin	Signalling	Prognostic marker in renal cancer (favorable)
86. PHB	Prohibitin	Signalling, DNA synthesis	Prognostic marker in head and neck cancer (unfavorable), renal cancer (favorable) and liver cancer (unfavorable)
87. SLMAP	Sarcolemma associated protein	Signalling	Prognostic marker in renal cancer (favorable) and lung cancer (unfavorable)
88. CALM3	Calmodulin 3	Signalling	Prognostic marker in lung cancer (unfavorable) and thyroid cancer (favorable)
89. RACK1	Receptor for activation C kinase 1	Cell cycle, Apoptosis, Translational regulation	Prognostic marker in liver cancer (unfavorable)
Miscellaneous			
90. SERPINC1	Serpin family C member 1	Thrombophilia	Prognostic marker in liver cancer (favorable)
91. SUMO4	Small ubiquitin-like modifier 4	Ubl conjugation pathway	Not prognostic

Gene name	Protein Name	Function	Relation to cancer
92. SUMO2	Small ubiquitin-like modifier 2	Ubl conjugation pathway	Prognostic marker in renal cancer (unfavorable), endometrial cancer (unfavorable) and liver cancer (unfavorable)
93. TLN1	Talin 1	Host-virus interaction	Prognostic marker in colorectal cancer (unfavorable) and renal cancer (favorable)
94. HPX	Hemopexin	Host-virus interaction	Prognostic marker in liver cancer (favourable)
95. PPIA	Peptidylprolyl isomerase A	Host-virus interaction	Prognostic marker in liver cancer (unfavorable)
96. CDC42	Cell division cycle 42,	Mental retardation	Prognostic marker in liver cancer (unfavorable)
97. CALR	Calreticulin	Calcium, Zinc-binding, Cancer related	Prognostic marker in renal cancer (unfavorable) and ovarian cancer (favorable)
98. CTSD	Cathepsin D	Proteolysis	Prognostic marker in renal cancer (unfavourable) and colorectal cancer (unfavorable)
99. CP	Ceruloplasmin	Ion transport	Prognostic marker in renal cancer (unfavourable)
100. TMEM109	Transmembrane protein 109	Ion transport	Prognostic marker in urothelial cancer (unfavourable)
101. SPYL1	Shynaptophysin like 1	Transport	Prognostic marker in renal cancer (favourable)
102. SIX5	SIX homeobox 5	Transcription	Not prognostic
103. PCYOX1	Preylcysteine oxidase 1	Ion transport, Protein catabolism	Prognostic marker in renal cancer (favourable)
104. POTEE	POTE ankyrin domain family member E	Extracellular protein	Not prognostic

Discussion

With the advent of tools of genomics and proteomics, a surprising level of heterogeneity has been found in malignant tumours. It is now widely accepted that solid tumours often comprise of distinct subpopulations of transformed cells with unique physiology [30]. Nevertheless, certain characteristics viz., dedifferentiation, metabolic reprogramming, attainment of unlimited proliferation potential, lack of response to the growth-inhibitory signals, evasion of apoptosis, tissue invasion etc.; make cancer cells highly distinguishable from their normal counterparts. Despite significant advancements in understanding the biology of cancer, due to such complexities; identification of novel therapeutic targets remains a challenge [31].

In recent years, Striatin has gained significant attention for its role in cancer in general and in hippo signalling in particular [4–6]. The role of its paralogue SG2NA in the context of cancer or any other diseases is rather obscure. Unlike Striatin, that has higher level of expression in the striatum region of the brain (and named accordingly), the expression of SG2NA is ubiquitous. It also has several splice variants with complex subcellular distributions [15, 20]. Therefore, the interacting partners of SG2NA are likely to be highly diverse. In agreement, by co-immunoprecipitation and blue-native PAGE analyses, we have recently found that in rat midbrain extract SG2NA has ~ 200 interacting partners and three fourth of which also interact with the cancer associate protein DJ-1 (Manuscript under review in BBA Proteins and Proteomics). Proteins that interact with SG2NA are involved in a plethora of cellular pathways including metabolism, mitochondrial function, cell signalling etc. Since DJ-1 has been associated with the bladder, prostate, colorectal and gastric cancers etc. [32, 33], it is anticipated that SG2NA and some of its associated proteins would also be involved in cancer. Such notion is further strengthened by our recent observation that overexpression of 35 kDa SG2NA and knocking down the 78 kDa in NIH3T3 cells induces certain markers of epithelial to mesenchymal transition [21]. To explore the possible role of SG2NAs in tumour progression, we first tested its expression profile in several well-established cancer cell lines. It appears from the results that rather than having an exclusive profile of expression in those cells, it was highly variable among the cell lines originating from different types of tumours. Further, in several cell lines, there were major disconnect between the mRNA and protein levels, suggesting a dynamic regulation of its expression. Similarly, its expression profile not only varied among three different cancer tissues we had tested, it also varied between the stages of breast cancers. Considering the large number of interacting partners of SG2NA (seen in mid-brain), it thus appears that rather than being involved in a few selective pathways, it might be dynamically engaged in more innate cellular networks. In agreement, coimmunoprecipitation analyses showed that while there are several hundred interacting partners of SG2NA common between both normal and tumour cells, there are also eighty-two proteins of diverse functions that interact with it only in tumour cells. Although these proteins are functionally diverse, we clustered them based on their functions viz., protein synthesis and ribosomal structure (21 proteins); chaperone & heat shock proteins (5 proteins); transporters (5 proteins); GTP binding tubulins (11 proteins); cell signalling (3 proteins); binding to DNA/RNA (5 proteins); glycolysis (7 proteins); complement pathway (5 proteins); structural proteins (5 proteins) etc. Since several of these proteins are part of multimeric assemblies like ribosome and microtubules, some might have been immunoprecipitated along with others which directly interact with SG2NA. Therefore, even if we accept

that all those eighty-two proteins are not necessarily the unique interacting partners of SG2NA, most turned out to be the prognostic markers of various types of cancers. It thus strongly suggests that SG2NA is involved in modulating a plethora of cellular pathways, and while transiting from normal to cancer phenotype; it partially switches its interacting partners to facilitate the reprogramming of the cellular events, tuning it towards tumour progression. Though our inference is based on some preliminary studies, it nonetheless advocates nuanced role of SG2NA in normal cell function as well as tumorigenesis.

Declarations

Acknowledgements:

The authors thankfully acknowledge funding support from the Department of Biotechnology, Government of India [BT/ PR22963/MED/122/76/2017] awarded to SKG. PB is a recipient of Junior/Senior Research Fellowship from the CSIR, Government of India.

Conflict of Interest:

No conflict of interest.

Credit Author Statement:

Buddhi Prakash Jain initiated the work and performed experiments for Figure 1 and 2. He also did bioinformatic analysis part for Figure 4. Padmini Bisoyi performed the experiments for the Figure 3 and 4. Padmalaya Devi collected the cancer tissue samples and helped in their analysis. Kusumbati Besra did the histopathological analysis of the samples. Anamika Prasad helped in the western blot and cell culture work. Shyamal Goswami generated the overall idea of the manuscript and wrote the manuscript. Buddhi Prakash Jain and Padmini Bisoyi helped in writing.

Data availability:

All data generated and analysed during the study are included in the manuscript.

References

1. Chen C, Shi Z, Zhang W et al (2014) Striatins contain a noncanonical coiled coil that binds protein phosphatase 2A A subunit to form a 2:2 heterotetrameric core of striatin-interacting phosphatase and kinase (STRIPAK) complex. *J Biol Chem* 289:9651–9661. <https://doi.org/10.1074/jbc.M113.529297>
2. Jain BP, Pandey S (2018) WD40 Repeat Proteins: Signalling Scaffold with Diverse Functions. *Protein J* 37:391–406. <https://doi.org/10.1007/s10930-018-9785-7>
3. Kück U, Radchenko D, Teichert I (2019) STRIPAK, a highly conserved signaling complex, controls multiple eukaryotic cellular and developmental processes and is linked with human diseases. *Biol*

Chem. <https://doi.org/10.1515/hsz-2019-0173>

4. Shi Z, Jiao S, Zhou Z (2016) STRIPAK complexes in cell signaling and cancer. *Oncogene* 35:4549–4557. <https://doi.org/10.1038/onc.2016.9>
5. Tang Y, Chen M, Zhou L et al (2019) Architecture, substructures, and dynamic assembly of STRIPAK complexes in Hippo signaling. *Cell Discov* 5:3. <https://doi.org/10.1038/s41421-018-0077-3>
6. Xie R, Wen F, Qin Y (2020) The Dysregulation and Prognostic Analysis of STRIPAK Complex Across Cancers. *Front Cell Dev Biol* 8:625. <https://doi.org/10.3389/fcell.2020.00625>
7. Moreno CS, Park S, Nelson K et al (2000) WD40 repeat proteins striatin and S/G(2) nuclear autoantigen are members of a novel family of calmodulin-binding proteins that associate with protein phosphatase 2A. *J Biol Chem* 275:5257–5263
8. Neal SJ, Zhou Q, Pignoni F (2020) STRIPAK-PP2A regulates Hippo-Yorkie signaling to suppress retinal fate in the *Drosophila* eye disc peripodial epithelium. *J Cell Sci* 133. <https://doi.org/10.1242/jcs.237834>
9. Chen M, Zhang H, Shi Z et al (2018) The MST4-MOB4 complex disrupts the MST1-MOB1 complex in the Hippo-YAP pathway and plays a pro-oncogenic role in pancreatic cancer. *J Biol Chem* 293:14455–14469. <https://doi.org/10.1074/jbc.RA118.003279>
10. Jin X, Zhu L, Xiao S et al (2021) MST1 inhibits the progression of breast cancer by regulating the Hippo signaling pathway and may serve as a prognostic biomarker. *Mol Med Rep* 23. <https://doi.org/10.3892/mmr.2021.12022>
11. Lin Z-H, Wang L, Zhang J-B et al (2014) MST4 promotes hepatocellular carcinoma epithelial-mesenchymal transition and metastasis via activation of the p-ERK pathway. *Int J Oncol* 45:629–640. <https://doi.org/10.3892/ijo.2014.2455>
12. Hwang J, Pallas DC (2014) STRIPAK complexes: structure, biological function, and involvement in human diseases. *Int J Biochem Cell Biol* 47:118–148. <https://doi.org/10.1016/j.biocel.2013.11.021>
13. Chen Y-K, Chen C-Y, Hu H-T, Hsueh Y-P (2012) CTTNBP2, but not CTTNBP2NL, regulates dendritic spinogenesis and synaptic distribution of the striatin-PP2A complex. *Mol Biol Cell* 23:4383–4392. <https://doi.org/10.1091/mbc.E12-05-0365>
14. Muro Y, Chan EK, Landberg G, Tan EM (1995) A cell-cycle nuclear autoantigen containing WD-40 motifs expressed mainly in S and G2 phase cells. *Biochem Biophys Res Commun* 207:1029–1037. <https://doi.org/10.1006/bbrc.1995.1288>
15. Jain BP, Chauhan P, Tanti GK et al (2015) Tissue specific expression of SG2NA is regulated by differential splicing, RNA editing and differential polyadenylation. *Gene* 556:119–126. <https://doi.org/10.1016/j.gene.2014.11.045>
16. Soni S, Tyagi C, Grover A, Goswami SK (2014) Molecular modeling and molecular dynamics simulations based structural analysis of the SG2NA protein variants. *BMC Res Notes* 7:446. <https://doi.org/10.1186/1756-0500-7-446>
17. Tanti GK, Singarapu N, Muthuswami R, Goswami SK (2014) Among the three striatin family members, SG2NA was first to arise during evolution. *Front Biosci Sch Ed* 6:1–15.

<https://doi.org/10.2741/s409>

18. Sanghamitra M, Talukder I, Singarapu N et al (2008) WD-40 repeat protein SG2NA has multiple splice variants with tissue restricted and growth responsive properties. *Gene* 420:48–56.
<https://doi.org/10.1016/j.gene.2008.04.016>
19. Tanti GK, Pandey S, Goswami SK (2015) SG2NA enhances cancer cell survival by stabilizing DJ-1 and thus activating Akt. *Biochem Biophys Res Commun* 463:524–531.
<https://doi.org/10.1016/j.bbrc.2015.05.069>
20. Chauhan P, Gupta R, Jain BP et al (2020) Subcellular dynamics of variants of SG2NA in NIH3T3 fibroblasts. *Cell Biol Int* 44:637–650. <https://doi.org/10.1002/cbin.11264>
21. Gupta R, Kumar G, Jain BP et al (2021) Ectopic expression of 35 kDa and knocking down of 78 kDa SG2NAs induce cytoskeletal reorganization, alter membrane sialylation, and modulate the markers of EMT. *Mol Cell Biochem* 476:633–648. <https://doi.org/10.1007/s11010-020-03932-2>
22. Tanti GK, Goswami SK (2014) SG2NA recruits DJ-1 and Akt into the mitochondria and membrane to protect cells from oxidative damage. *Free Radic Biol Med* 75:1–13.
<https://doi.org/10.1016/j.freeradbiomed.2014.07.009>
23. Jain BP, Pandey S, Saleem N et al (2017) SG2NA is a regulator of endoplasmic reticulum (ER) homeostasis as its depletion leads to ER stress. *Cell Stress Chaperones* 22:853–866.
<https://doi.org/10.1007/s12192-017-0816-7>
24. Pandey S, Talukdar I, Jain BP et al (2017) GSK3 β and ERK regulate the expression of 78 kDa SG2NA and ectopic modulation of its level affects phases of cell cycle. *Sci Rep* 7:7555.
<https://doi.org/10.1038/s41598-017-08085-9>
25. Hulsen T, de Vlieg J, Alkema W (2008) BioVenn - a web application for the comparison and visualization of biological lists using area-proportional Venn diagrams. *BMC Genomics* 9:488.
<https://doi.org/10.1186/1471-2164-9-488>
26. Huang DW, Sherman BT, Lempicki RA (2009) Systematic and integrative analysis of large gene lists using DAVID bioinformatics resources. *Nat Protoc* 4:44–57. <https://doi.org/10.1038/nprot.2008.211>
27. Huang DW, Sherman BT, Lempicki RA (2009) Bioinformatics enrichment tools: paths toward the comprehensive functional analysis of large gene lists. *Nucleic Acids Res* 37:1–13.
<https://doi.org/10.1093/nar/gkn923>
28. Kurosaki T, Maquat LE (2016) Nonsense-mediated mRNA decay in humans at a glance. *J Cell Sci* 129:461–467. <https://doi.org/10.1242/jcs.181008>
29. Popp MW-L, Maquat LE (2013) Organizing principles of mammalian nonsense-mediated mRNA decay. *Annu Rev Genet* 47:139–165. <https://doi.org/10.1146/annurev-genet-111212-133424>
30. Dagogo-Jack I, Shaw AT (2018) Tumour heterogeneity and resistance to cancer therapies. *Nat Rev Clin Oncol* 15:81–94. <https://doi.org/10.1038/nrclinonc.2017.166>
31. Lewis SM, Asselin-Labat M-L, Nguyen Q et al (2021) Spatial omics and multiplexed imaging to explore cancer biology. *Nat Methods* 18:997–1012. <https://doi.org/10.1038/s41592-021-01203-6>

32. Kim J-Y, Kim H-J, Jung C-W et al (2021) PARK7 maintains the stemness of glioblastoma stem cells by stabilizing epidermal growth factor receptor variant III. *Oncogene* 40:508–521. <https://doi.org/10.1038/s41388-020-01543-1>
33. Zhang L, Wang J, Wang J et al (2020) Role of DJ-1 in Immune and Inflammatory Diseases. *Front Immunol* 11:994. <https://doi.org/10.3389/fimmu.2020.00994>

Figures

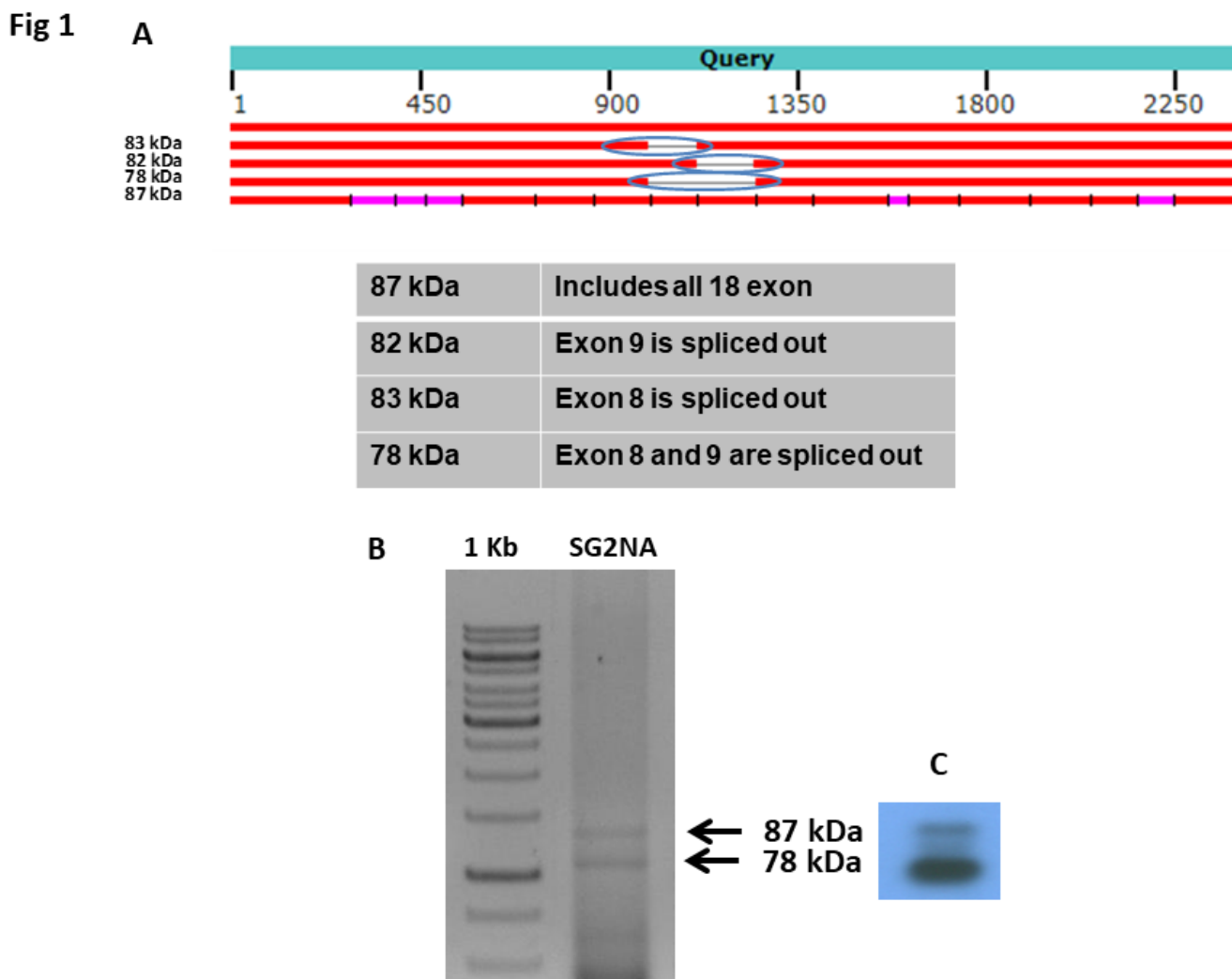


Figure 1

Identification of the human isoforms of SG2NA: (A) To identify splice variants of human SG2NA, full length human SG2NA ORF was retrieved from the NCBI data base (Nucleotides) and used for searching (BLAST) the EST database in the NCBI. Splice variants generated by alternative splicing at exons 8 and 9 are encircled. (B) Total RNA was isolated from HEK293T cell line, converted into cDNA and amplified using primer pair flanking the splice region i.e., exon 8 and 9 (primer pair: Exon 5 forward and Exon 15 Reverse). The amplified product was resolved on 1% agarose. Two bands obtained whose length

corroborated with the 78 and 87 kDa isoforms. (C) The amplified products were confirmed by southern blotting using human SG2NA clone as probe.

Fig 2

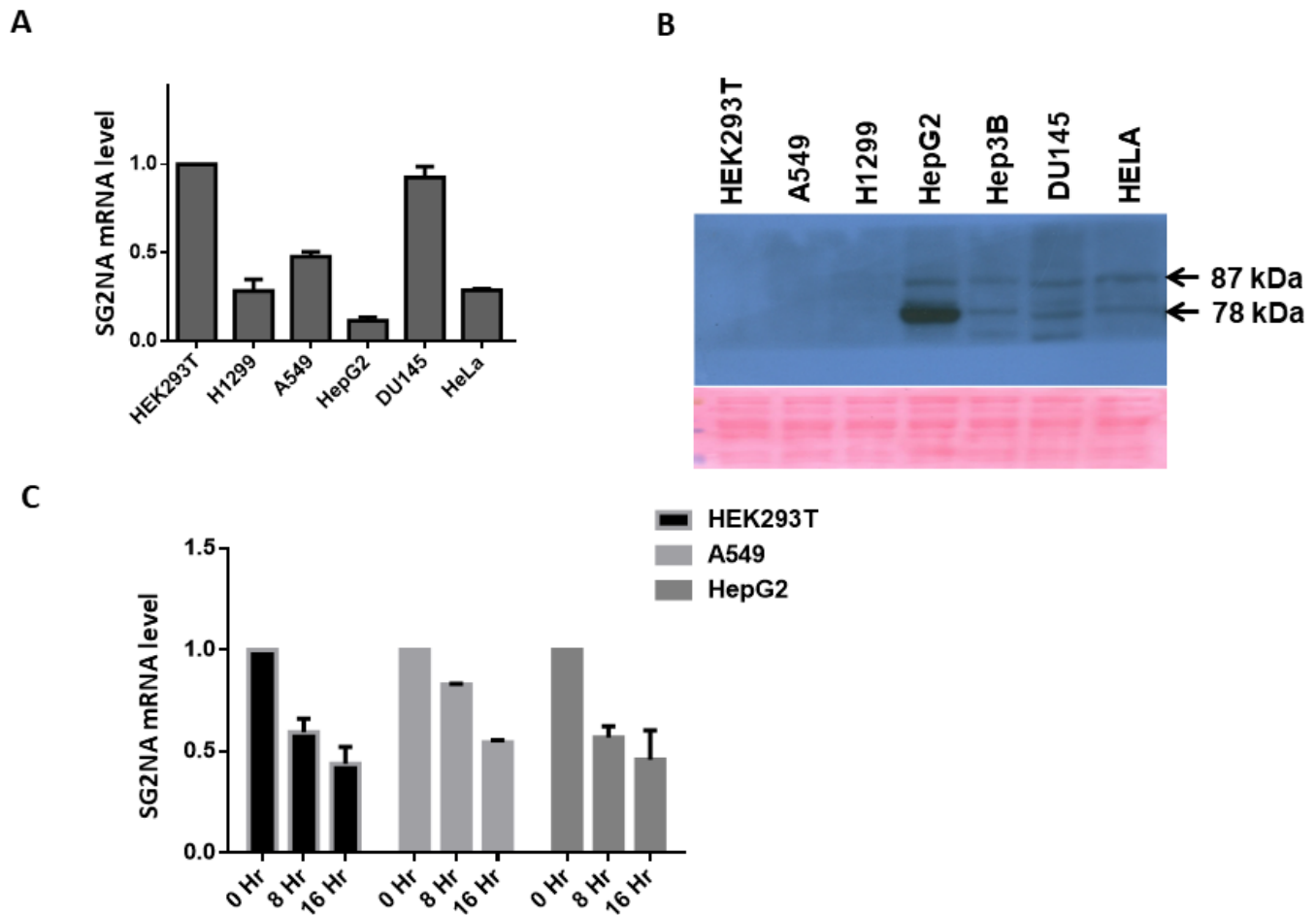


Figure 2

Expression profile of SG2NA in Cancer cell lines: (A) Total RNA was isolated from the different cancer cell lines and analysed for the relative mRNA levels (normalized against β actin) for sg2na by real time PCR using primer pairs from the ORF and the 3'UTR. (B) Total protein was isolated from different cancer cell lines viz., HEK293T, A549, H1299, HepG2, Hep3B, DU145, HELA, C6, resolved on 10% SDS-PAGE and blotted with SG2NA antibody. (C) To check the stability of sg2na mRNA in different cancer cell lines, HEK293T, A549 and HepG2 cells were treated with actinomycin D (10 μ g/ml) to stop transcription. Cells were then harvested at 0, 8 and 16 hr and realtime PCR analysis was done using sg2na transcript specific primer pair.

Fig 3

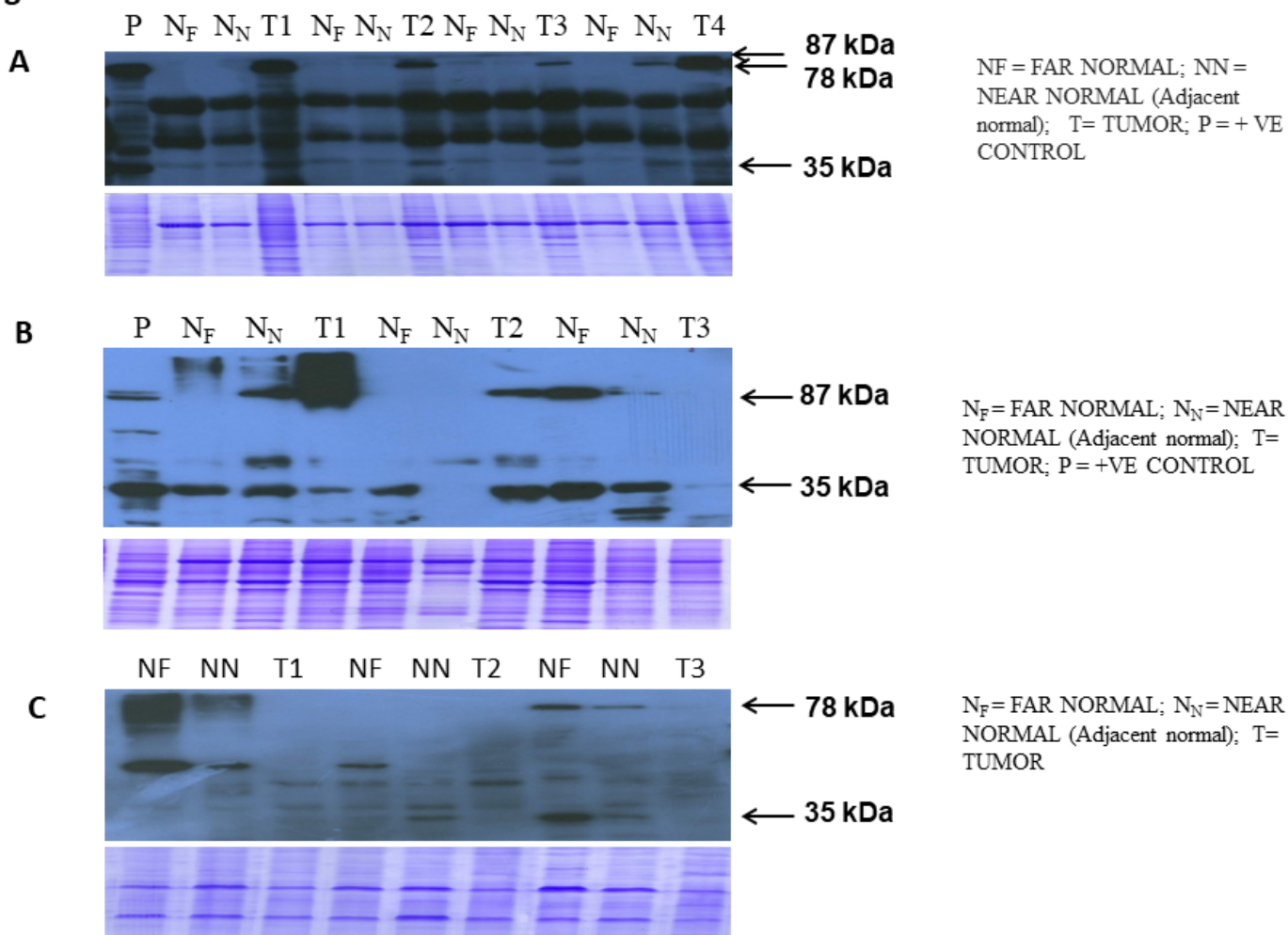


Figure 3

Expression profile of SG2NA isoforms in different cancer tissue vs control: Differential expression of SG2NA between tumor and normal human tissues. Total protein (70µg) was isolated from different patient tissues viz., breast, stomach, colon (A, B, and C respectively), resolved on 10% SDS-PAGE and blotted with SG2NA antibody respectively.

Fig 4

No of proteins interacting with SG2NA in	
Breast tumor only	104
Normal breast tissue	28
Common between normal breast tissue and breast tumor tissue	187

SG2NA interactome
Breast Cancer vs Normal Tissue

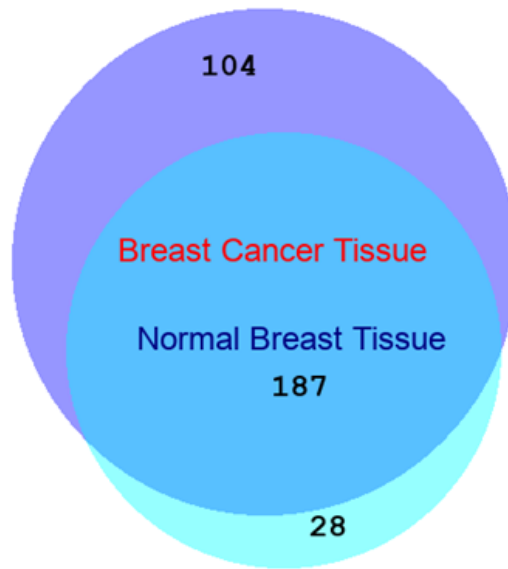


Figure 4

SG2NA interactome in Breast tumor and adjacent normal tissue: Table shows the number of interacting proteins of SG2NA in breast tumor tissue as well as adjacent normal breast tissue. Co-immunoprecipitation of control breast tissue and breast tumor tissue extract with SG2NA antibody identified total 215 proteins in control breast tissue and 291 proteins in breast tumor tissue. Total 187 proteins were found common between two datasets. Venn diagram showing SG2NA interacting proteins as identified by the Co-immunoprecipitation (details given in S1A).

Supplementary Files

This is a list of supplementary files associated with this preprint. Click to download.

- [SupplementaltableS1.xlsx](#)
- [SupplementaltableS2.xlsx](#)
- [SupplementaltableS3.xlsx](#)

- [SupplementaltableS4.docx](#)